Computational Insights into the Energetics of Single C_2-C_{10} Aliphatic Moieties Adsorbed on Hydrogenated Silicon (111) Surface

Francesco Buonocore,[a)] Sara Marchio, Simone Giusepponi, Massimo Celino

Italian National Agency for New Technologies, Energy and Sustainable Economic Development (ENEA) − C. R. Casaccia, Via Anguillarese 301, 00123 Rome, Italy

Abstract. Silicon's versatility as a semiconductor renders it indispensable across various domains, including electronics, sensors, and photovoltaics. Modifying Hydrogen-terminated Silicon surfaces with moieties adsorption offers a method to tailor the material's properties for specific applications. In this study, we employ ab initio density functional theory calculations to explore the energetics of single alkyl, 1-alkenyl and 1-alkynyl moieties chemisorbed on Hydrogen-terminated Silicon (111) surface. We analyse the interfacial dipole induced by Si–C bond formation that determines the Schottky barrier and examine the alignment of the frontier orbitals energy levels with Silicon band structure to investigate the charge transfer based on tunnelling mechanism. Our findings provide valuable insights into how aliphatic moiety functionalization affects interfacial electronic properties, offering clues for optimizing Silicon-based devices.

I. INTRODUCTION

Silicon, with its exceptional semiconductor properties, is a fundamental material in modern technology, underpinning a vast array of applications from integrated circuits and sensors to photovoltaic cells. [1-13] The versatility and efficiency of Silicon-based devices are significantly enhanced by surface modifications, which allow for precise tuning of electronic, optical, and chemical properties. Unfortunately, the presence of Silicon oxide during the fabrication processes leads to lower quality or non-functioning devices. Indeed, Silicon oxide constitutes an insulating layer that must be prevented when electrical contact is formed. One of the most adopted strategies to avoid oxide formation involves the functionalization of Hydrogen-terminated Silicon (H−Si) surfaces with molecular monolayers. [14] Actually, there is a growing interest in developing alternative functionalization methods that avoid oxide formation, thereby preserving the conductive properties of Silicon. Since the first report of Si–C alkyl monolayers, [15] the Si−C bond has been proved to be more stable than Si−H bond. In this context, the aliphatic chain molecules represent a convincing option to prevent the formation of undesired oxide on the Si surface, creating a direct interface that maintains

[a)] Author to whom correspondence should be addressed. Electronic mail: francesco.buonocore@enea.it.

desirable conductive properties. This technique enables the customization of surface characteristics to meet the specific demands of various applications. Moreover, the formation of molecular monolayers based on aliphatic chains has been proposed [16] to improve the performance of low-cost polycrystalline semiconductors. The impact of such functionalization on the electronic structure and interfacial properties of Silicon, however, requires thorough investigation.

Short aliphatic chains are known to form more ordered monolayers than longer ones. [17-18] However, monolayers derived from short alkenes and alkynes are more difficult to synthesise using wet chemistry. For this reason, different approaches using gaseous aliphatic molecules at elevated pressure have been proposed. [18]

Several theoretical studies have been dedicated to the functionalization of Hydrogen-terminated Silicon (111) (H−Si(111)) surface by aliphatic chains. Zhang and co-authors have investigated the optimal packing structure of C_{18} alkyl monolayers on a Si(111) surface based on molecular dynamics simulations. [19] In this work, the aliphatic chains are generically indicated as C_N, where N represents the number of C atoms. The morphology of alkyl monolayers from C_2 to C_{18} on the H−Si(111) surface was investigated by molecular simulation method. [20] Numerous works have been based on ab initio density functional theory (DFT). The binding energies of 1-alkenes and 1-alkynes to the H−Si surface were calculated to determine the thermodynamic feasibility of the monolayer structures. It was demonstrated that coverage as high as 75% is possible for octadecenyl chains due to the significantly larger reaction exothermicity of the 1-alkynes. [21] The functionalization of hydrogenated Si surface with C_{18} alkyl monolayers to form hydrophobic coatings was explored. [22] The sequence of the stability of C_N alkyls with N ranging from 1 to 10 for different linkers was assessed. [23] Ab initio calculations were performed to investigate the reactivity of Silicon terminated with aliphatic chains toward oxidizing molecules to understand the mechanisms that avoid the oxidation of the Silicon substrate. [24] Moreover, the workfunction of H−Si(111) was shown to be modified over a range of 1.7 eV through the adsorption of C_N alkyl monolayers with N ranging from 1 to 14. [25]

This study utilizes ab initio DFT calculations to investigate the effects of single aliphatic chain moiety adsorption on the energetics of H–Si(111) surfaces. We calculated using DFT the minimal energy geometrical configurations of alkyl (C_NH_{2N+1}), 1-alkenyl (C_NH_{N+1}) and 1-alkynyl (C_2H_1, C_NH_{2N-3} for N>2) moieties, the number of Carbon atoms N varying from 2 to 10, adsorbed on surface. It has been reported that the functionalization with 1-alkenes and 1-alkynes of H−Si(111) surface results with the formation of alkyl and 1-alkenyl monolayers, respectively. [26] However, this work adopts a broader perspective to investigate the distinct effects that single, double, or triple C−C bonds near the surface in individual aliphatic moieties have on the energetics of the inorganic/organic interface. These effects are analysed in the context of replacing one H atom attached to Si surface with the aliphatic moiety, resulting in the substitution of one Si–H bond with a Si–C bond, and the chemisorption of the moiety. By examining the charge distribution, the dipole formation, and the alignment of molecular energy levels at the Si–C interface, our research seeks to provide a detailed understanding of how these modifications influence interface properties such as Schottky and tunnelling barriers, offering valuable insights for optimizing design and functionality of Silicon-based devices. The investigation of single moiety adsorption is a prelude to further studies where the interactions among moieties in monolayer will be explored.

II. THEORETICAL METHODS

The computational approach was based on DFT and pseudo-potential plane-wave method using PWSCF code as implemented in the QUANTUM-ESPRESSO package. [27-28] To account for Van der Waals interactions, we employed the nonlocal DFT functional VdW-df-cx, [29] which has been previously employed to investigate charge transfer at the Silicon–organic interface. [30]

The pseudo-potential plane-wave calculations were performed using ultrasoft pseudo-potentials. [31] All the relax calculations were performed with cut-off for the wave functions of 40 Ry and 2×2×1 Monkhorst-Pack grid. We allowed a convergence of the total energy below 0.0001 Ry/atom. The systems were fully relaxed with a convergence threshold of 0.001 Ryd/Å on the inter-atomic forces. The electronic structure calculations of the density of states (DOS) converged with 8×8×1 Monkhorst-Pack mesh of k-points.

We characterized the interfacial energetics of molecules ranging from C_2 to C_{10} with single, double, and triple C−C bonds near the H−Si(111) surface. Specifically, we examined alkyl moieties (C_NH_{2N+1}) containing only single C−C bonds, 1-alkenyl moieties (C_NH_{N+1}) with the first C−C bond near the surface being a double bond followed by alternating single and double bonds, and 1-alkynyl moieties (C_2H_1, C_NH_{2N-3} for N>2) where the first C−C bond near the surface is a triple bond, with the remaining C−C bonds being single.

The possible structural configurations of moiety's adsorption onto the Si surface have been systematically explored by adopting a five bilayers slab supercell model. The five bilayers Si(111) slab is thick 15 Å; the box dimension perpendicular to the slab is set to L_z = 50 Å creating a vacuum space to prevent interaction with adjacent images. The remaining dimensions are set to $L_x = L_y$ = 15 Å. One moiety adsorbed per supercell corresponds to a density of 8.9×10^{-19} molecules/cm^2.

The most stable configurations on the five bilayers slab (Figures S1-S3) have been used for an eight bilayers slab supercell model (Figures 1a-b) to calculate the dipole variation with respect to the full hydrogenated surface upon relax of the extended structure. The eight bilayers Si(111) slab is thick 23 Å; the box dimension perpendicular to the slab is set to L_z = 65 Å, and the remaining dimensions are set to the same than for the five bilayers slab. The chosen number of bilayers in both cases is a compromise between computational time and accuracy. The five bilayers slab model is computationally cheaper and allowed to explore many adsorption configurations. The slab models we used are asymmetric. Indeed, in the five bilayers slab, the H atoms and the moiety were only adsorbed over the top layer, and the two bottom bilayers were fixed in the bulk positions (the bottom surface is clean); in the eight bilayers slab, the top and the bottom layers were passivated by H atoms, the moiety was adsorbed over the top layer, and the two bilayers in the middle were fixed in the bulk positions. This required the correction for dipole self-interactions in the calculations. [32]

We calculated the total dipole along z direction (perpendicular to the surface) of a system in the supercell as:

$$P_z(\text{system}) = \int_0^L z \cdot \bar{\rho}(z) dz \qquad (1),$$

where $\bar{\rho}(z)$ is the xy-plane integrated total charge density and L is the height of the supercell. We introduce the dipole ΔP_z that is the variation with respect to the fully H-passivated surface

of the dipole along z direction in consequence of the desorption of one H atom and the adsorption of the moiety. We calculate ΔP_z as the difference of the dipole $P_{z,TOP}$ on the top surface (moiety chemisorbed on H-passivated surface with substitution of one H atom) and the dipole $P_{z,BOTTOM}$ of the bottom surface (fully H-passivated surface) projected along z direction of the eight bilayers slab. Therefore:

$$\Delta P_z = P_{z,TOP} - P_{z,BOTTOM} \qquad (2),$$

where the $P_{z,TOP}$ and $P_{z,BOTTOM}$ dipoles are illustrated in Figure 1c. Using the equation (1), it results that:

$$\Delta P_z = P_z(slab+H^*+moiety) \qquad (3),$$

where the slab+H^*+moiety system is the supercell of the hydrogenated eight bilayers slab with moiety adsorbed on top, shown in Figure 1. The symbol H^* means that one H has been removed from the adsorption site; e.g., slab+H^* is the system (without the moiety) where all Si sites on the surface but the adsorption site are passivated with H. Therefore, the equations (1) and (3) allow to calculate how much the dipole of the moiety adsorbed on the H-passivated surface changes with respect to the dipole of the fully H-passivated surface. On the other side, ΔP_{mol} is the difference of the dipole of the moiety dipole bound to the surface in the full system, calculated as $P_z(slab+H^*+moiety)$-$P_z(slab+H^*)$, and the dipole $P_z(moiety)$ of the isolated molecule, frozen in the geometry of adsorption. The dipole ΔP_{mol} quantifies the effect of the formation of the Si−C bond on the molecule, therefore it is the dipole associated to the molecule-substrate bond. The positivity of ΔP_{mol} means an increase of the dipole of the molecule following the adsorption. Of course, the surface dipole is influenced by the tilting angle, which in turn depends on the specific adsorbate, as detailed in the following section on geometric structure.

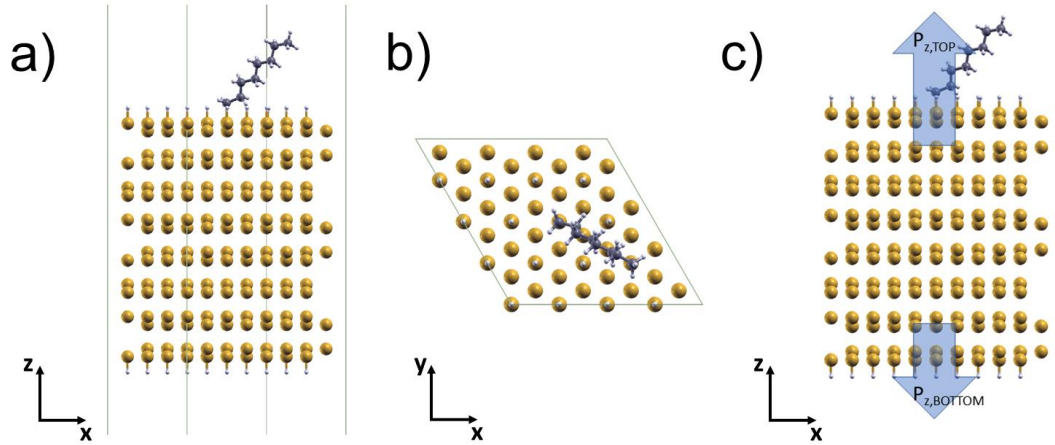

Figure 1. a) Side and b) top view of the eight bilayers H−Si(111) slab model with adsorption of C_N moiety on the top surface. In c) the dipoles associated to the bottom and top surfaces are shown. In this example, C_8 alkyl moiety is adsorbed. Yellow, white, and grey spheres are Si, H and C atoms, respectively.

III. RESULTS AND DISCUSSION

A. Geometric structure

We screened a wide range of possible adhesion configurations of molecules with single, double, and triple Carbon-Carbon bonds attached to the H−Si(111) surface and performed the structural optimization of each of them. In the present work, we report the geometry corresponding to the minimal energy of adhesion for which ones we have proceeded to the characterization of the electronic properties. We computed the molecule-surface dissociation energy as $E_d = (E_m + E_s) - E_{sm}$, where E_{sm} is the energy of the system with the molecule grafted onto the surface, and E_m and E_s are the energy of the isolated molecule and the surface, respectively. For each minimal energy configuration, structural characterization was conducted by calculating geometric parameters including the bond distance d(**C_1C_2**) between the two Carbon atoms closest to the surface and their respective bond angle θ(**C_1C_2**) with respect to the z-axis, the Carbon-Silicon bond distance d(**C_1Si**) and the molecular axis bond angle with respect to the z-axis θ(**C_1C_N**), along with the molecule's rotation angle φ in the xy plane (atomic labels and geometric parameters are referred in Figure 2). The values obtained are summarized in Table 1. In the following, the tilting angle θ(**C_1C_N**) is also referred simply as the tilting angle. The description of the workflow process, and the geometric structure parameters of the screened configurations can be found in the dataset available on reference [33].

Table 1. Geometric parameters of the aliphatic moieties adsorbed on the H−Si(111) surface. Refer to Figure 2 for the meaning of the listed parameters and atomic labels.

Moiety	d(**C_1C_2**)	d(**C_1Si**)	θ(**C_1C_N**)	θ(**C_1C_2**)	φ	Dissociation energy (eV)	Group type
$C_{10}H_{21}$	1.526	1.904	36.32	64.02	14.77	3.827	Alkyl
C_8H_{17}	1.529	1.905	36.41	62.09	119.01	3.829	Alkyl
C_6H_{13}	1.527	1.906	48.16	68.02	134.12	3.791	Alkyl
C_4H_9	1.528	1.907	42.34	62.51	141.83	3.792	Alkyl
C_2H_5	1.529	1.910	57.79	57.79	109.92	3.761	Alkyl
$C_{10}H_{11}$	1.360	1.860	34.76	56.35	72.02	4.505	1-alkenyl
C_8H_9	1.358	1.858	34.95	55.56	59.35	4.496	1-alkenyl
C_6H_7	1.357	1.864	41.15	59.47	169.68	4.449	1-alkenyl
C_4H_5	1.352	1.864	40.86	57.57	179.95	4.498	1-alkenyl
C_2H_3	1.339	1.873	50.54	50.54	174.95	4.204	1-alkenyl
$C_{10}H_{17}$	1.225	1.816	67.19	24.75	104.08	5.536	1-alkynyl
C_8H_{13}	1.224	1.813	58.78	22.82	46.57	5.462	1-alkynyl
C_6H_9	1.223	1.811	37.74	16.53	119.10	5.442	1-alkynyl
C_4H_5	1.223	1.812	35.48	9.25	148.46	5.415	1-alkynyl
C_2H	1.219	1.824	1.98	1.98	150.82	5.506	1-alkynyl

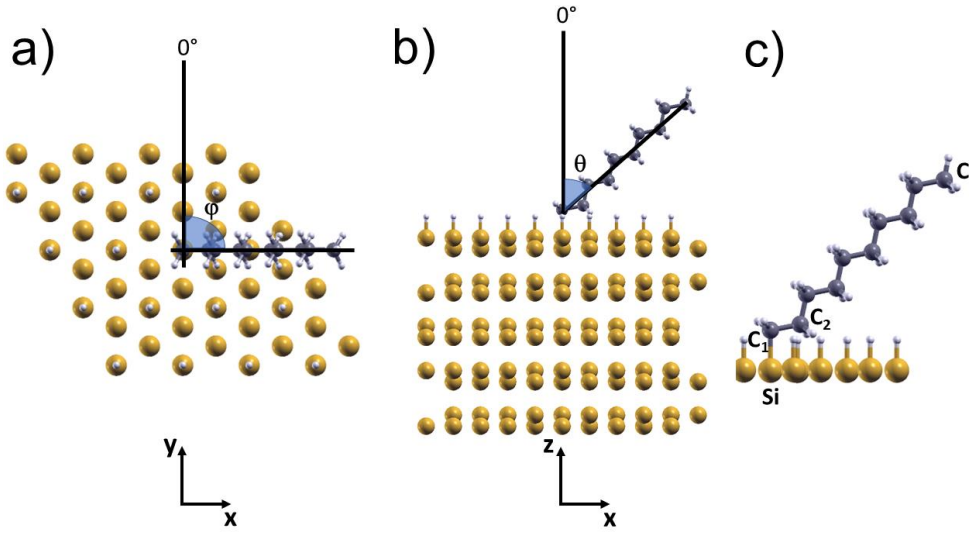

Figure 2. (a) Top and (b) side views of the H−Si(111) five bilayers slab with an adsorbed aliphatic chain. The geometrical parameters φ and θ are indicated. (c) Detailed representation showing the $\mathbf{C_1}$, $\mathbf{C_2}$, $\mathbf{C_N}$, and **Si** atoms. Yellow, white and grey spheres are Si, H and C atoms, respectively.

The d($\mathbf{C_1Si}$) and d($\mathbf{C_1C_2}$) bond lengths are decreasing in the following order: alkyl, 1-alkenyl, 1-alkynyl. To describe how the bond lengths change with respect to the group type, we can approximately state that d($\mathbf{C_1Si}$) ≈ 1.9, 1.85 and 1.8 Å and d($\mathbf{C_1C_2}$) ≈ 1.5, 1.35 and 1.2 Å for alkyl, 1-alkenyl and 1-alkynyl moieties, respectively.

The tilting angle of the alkyl and 1-alkenyl moieties $\mathbf{C_1C_2}$ bond between the two C atoms closest to the surface is always higher (i.e., more tilted) than that of the molecular axis $\mathbf{C_1C_N}$. For example, in the case of C_{10} chains, the alkyl moiety has θ($\mathbf{C_1C_2}$) = 64.02° and θ($\mathbf{C_1C_N}$) = 36.32°, and the 1-alkenyl moiety has θ($\mathbf{C_1C_2}$) = 56.35° and θ($\mathbf{C_1C_N}$) = 34.76°. The opposite happens for the 1-alkynyl moiety that has θ($\mathbf{C_1C_2}$) = 24.75° and θ($\mathbf{C_1C_N}$) = 67.19° for the C_{10} example. The tilting of the molecular axis $\mathbf{C_1C_N}$ of alkyl moieties smoothly changes with respect to the Carbon chain length for N > 2, then it is almost constant for N equals to 8 and 10 with θ($\mathbf{C_1C_N}$) ≈ 36°. The same holds for 1-alkenyl moieties, where θ($\mathbf{C_1C_N}$) reaches the value of 35° for N equals to 8 and 10. Instead, the tilting of 1-alkynyl moieties increases with respect to N with 2° < θ($\mathbf{C_1C_N}$) < 68°. In particular, the 1-alkynyl moieties show the following peculiar behaviour: the shortest Carbon chains are not very tilted in the sense that they are almost perpendicular to the surface, for example, θ($\mathbf{C_1C_N}$)= 2°, 35° and 38° (the lowest tilting angles) for C_2, C_4 and C_6, respectively; the longest Carbon chains of 1-alkynyl moieties have the highest tilting angle across the three chemical groups, for example, θ($\mathbf{C_1C_N}$)= 59° and 67° for C_8 and C_{10} chains, respectively. The trends of the tiling angle increasing with respect to N agrees with the findings of Yuan and co-authors. [20] We found a weak dependence of the total energy on the molecule's rotation angle φ in the xy plane.

The 1-alkynyl moieties have the higher dissociation energy, above 5.5 eV, followed by the 1-alkenyl moieties with dissociation energy between 4.2 (C_2H_3) and 4.5 ($C_{10}H_{11}$) eV. The alkyl moieties have the lower dissociation energy, around 3.8 eV.

B. Dipole formation and Schottky barriers

A surface dipole is generated when the aliphatic chain is adsorbed on the Silicon surface; the Si−C bond is formed, accompanied by charge transfer between the adsorbate and the surface. Considering the Pauling electronegativity of Si (1.90) and C (2.5), a net electron density would be expected around the Carbon atom of Si−C, so that a negative surface dipole (i.e., negative charge pointing outward and positive charge pointing inward) resulted. Instead, based on our calculations, we are going to show that the resulting surface dipole is positive and not negative as predicted from electronegativity considerations on the Si−C bond only. In the following we demonstrate that the effect of the Si–C bond formation on the whole chain must be considered to find the correct dipole.

The dipole ΔP_z formed upon the desorption of one H atom and the adsorption of the moiety has been calculated based on the equations (1) and (3). The energy steps ψ and ψ_{mol} associated to the dipoles ΔP_z and ΔP_{mol}, respectively, are expressed by the following equations: [34]

$$\psi = 4\pi \, \Delta P_z / A \qquad (4),$$

$$\psi_{mol} = 4\pi \, \Delta P_{mol} / A \qquad (5),$$

where A is the surface area of the supercell. The energy step ψ is the change of the work function induced by the dipole. By the equations (4) and (5) we see that the dipole expressed in eV is intimately related to the adsorbate density on the surface. Therefore, for a fixed value of the dipole, decreasing the surface per adsorbate we obtain higher energy step.

In the following, the surface dipole is quantified as the energy step ψ corresponding to one adsorbate per supercell. We found that the surface dipole of alkyl moieties, reported in Table 1, changes from 0.115 to 0.153 eV varying within a range as short as 0.038 eV, and from 0.103 to 0.324 eV for the 1-alkenyl moieties (Table 2), changing in a range of 0.221 eV. Therefore, increasing the length of the 1-alkenyl moieties from C_2 to C_{10} results in overall variation of the dipole five times larger than for alkyl moieties.

Table 1. Ab initio dipoles ΔP_z and ΔP_{mol}, the ψ and ψ_{mol} energy steps, and charge transfer of alkyl moieties adsorbed on the H−Si(111) surface. The energy steps refer to one moiety adsorbed per supercell (see text).

Chain	ΔP_z (D)	ψ (eV)	ΔP_{mol} (D)	ψ_{mol} (eV)	Charge Transfer (e)
C_2	0.633	0.115	0.707	0.129	0.12
C_4	0.775	0.141	0.582	0.106	0.12
C_6	0.826	0.150	0.577	0.105	0.12
C_8	0.823	0.150	0.521	0.095	0.11
C_{10}	0.839	0.153	0.454	0.083	0.11

Table 2. Ab initio dipoles ΔP_z and ΔP_{mol}, the ψ and ψ_{mol} energy steps, and charge transfer of 1-alkenyl moieties adsorbed on the H−Si(111) surface. The energy steps refer to one moiety adsorbed per supercell (see text).

Chain	ΔP_z (D)	ψ (eV)	ΔP_{mol} (D)	ψ_{mol} (eV)	Charge Transfer (e)
C_2	0.567	0.103	0.320	0.058	0.18
C_4	0.947	0.172	0.647	0.118	0.17
C_6	1.248	0.227	0.931	0.169	0.16
C_8	1.505	0.274	0.545	0.099	0.16
C_{10}	1.784	0.324	0.115	0.021	0.15

The dipole ΔP_{mol} of the alkyl moieties has small dependence on the length of molecules, indeed the energy step ψ_{mol} (calculated by the equation (5)) assumes values from 0.083 to 0.129 eV. This means a small increase of the molecular dipole upon adsorption. On the other side, ψ_{mol} of the 1-alkenyl moieties varies in a range from 0.021 to 0.169 eV wider than the one for alkyl moieties. This means that the double C−C bond induces a more pronounced molecular dipole response upon adsorption. The tilting angle varies within a narrow range of 15° for alkyl and 10° 1-alkenyl moieties, suggesting that its influence on dipole is minimal.

In contrast to alkyl and 1-alkenyl, the 1-alkynyl moieties exhibit a non-monotonic variation of the dipole (Table 3). Indeed, starting from the value of 0.112 eV of C_2H, ψ increases to 0.296 and 0.295 eV for C_4H_5 and C_6H_9, and then decreases to 0.264 and 0.257 eV for C_8H_{13} and $C_{10}H_{17}$, respectively. Therefore, ψ increases of 0.184 eV moving from C_2H to C_4H_5 1-alkynyls, and then it remains almost constant with respect to the length of the molecule, showing a variation of just 0.039 eV. However, the overall dipole variation of 0.184 eV for 1-alkynyls is comparable to that of 1-alkenyl moieties. In this case, the tilting angle $\theta(\mathbf{C_1C_N})$ varies in a wide range from 2° and 67° by increasing N, strongly influencing the dipole on the surface. It is useful to see how much the adsorption affects the dipole of the isolated moiety also for 1-alkynyl moieties. When we consider the dipole associated to the molecule-substrate bond, the dipole ΔP_{mol} of 1-alkynyl adsorbates changes with respect to N in the opposite direction of alkyl and 1-alkenyl moieties (Table 3). Indeed, ψ_{mol} is -0.118 and -0.160 eV for C_2H and $C_{10}H_{17}$ 1-alkynyl moieties, respectively, reaching the largest value of -0.214 eV for C_6H_9 1-alkynyl moiety. Therefore, the dipole of the 1-alkynyl moiety adsorbed on H−Si(111) decreases when compared to the same moiety considered as isolated. To understand this different behavior with respect to the other moiety group types the charge analysis is required.

Table 3. Ab initio dipoles ΔP_z and ΔP_{mol}, the ψ and ψ_{mol} energy steps, and charge transfer of 1-alkynyl moieties adsorbed on the H−Si(111) surface. The energy steps refer to one moiety adsorbed per supercell (see text).

Chain	ΔP_z (D)	ψ (eV)	ΔP_{mol} (D)	ψ_{mol} (eV)	Charge Transfer (e)
C_2	0.616	0.112	-0.650	-0.118	0.29
C_4	1.628	0.296	-1.044	-0.190	0.25
C_6	1.620	0.295	-1.179	-0.214	0.24
C_8	1.449	0.264	-1.021	-0.186	0.22
C_{10}	1.415	0.257	-0.881	-0.160	0.21

To better understand the interaction between the substrate and the aliphatic moiety, we have calculated Löwdin charges and the difference of the charge density. The negative charge transferred from the substate to the moiety is in the range 0.11−0.12 *e* for alkyl, 0.15−0.18 *e* for

1-alkenyl, and 0.21−0.29 *e* for 1-alkynyl moieties. As a rule, we found that the charge transfer increases with the order of the C−C bond close the surface. Indeed, the localization of the electrons increases with the bond order, as shown by the difference of the charge density in Figure 3c, where C_8 adsorbates are considered; we see that more negative charge is accumulated around the triple bond close to the surface of 1-alkynyls (the same considerations hold for 1-alkynyl chains with different N). This negative charge partially compensates the positive charge of the tail, and it causes the decrease of the dipole of 1-alkynyl moieties with respect to the isolated ones so that ΔP_{mol} is negative.

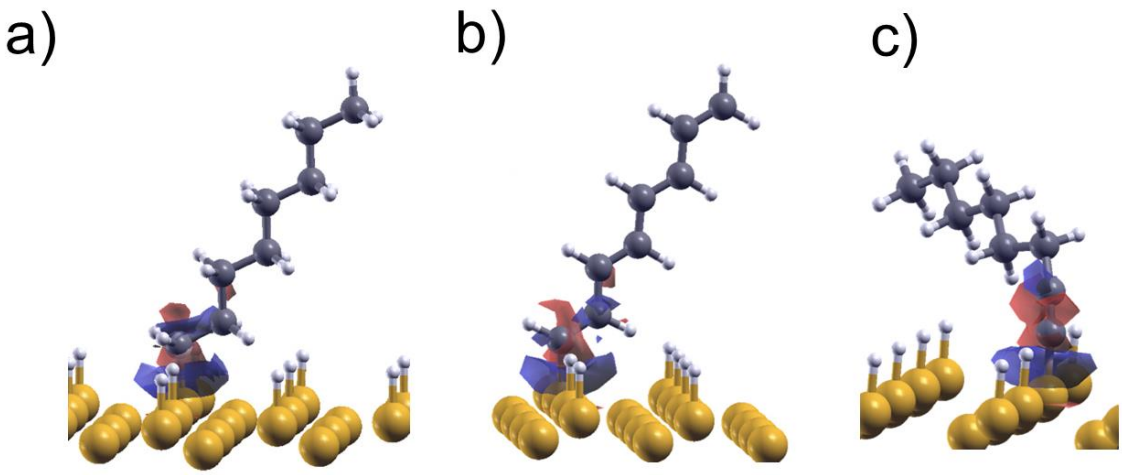

Figure 3. Difference of the charge density of a) alkyl, b) 1-alkenyl and c) 1-alkynyl C_8 moieties adsorbed on H−Si(111) surface (yellow, white and grey spheres are Si, H and C atoms, respectively; red and blue are negative and positive isosurfaces, respectively; isosurface value is ±0.003 a.u.).

To gain more insights into the charge distribution along the chain, we have plotted in Figures 4-8 the difference between the Löwdin and the neutral atomic charges as a function of the z coordinate, perpendicular to the surface, for chains ranging from C_2 to C_{10} of the three moieties groups. It is evident that a positive charge is localized on the top bilayer Si atom and negative charge is located on the atoms of the molecule close to the surface. The charge oscillates along the chain moving upwards along the moiety, then a positive charge is localized on the terminal group opposite to the surface. This distribution of charges results in the positive dipole (dipole pointing outwards). As we stated above, basic considerations based on Pauling electronegativity suggest that a net electron density accumulates near the Carbon atoms in the Si–C bond, resulting in the formation of a negative surface dipole. Indeed, the calculation of the Löwdin charges shows that negative charges move from the surface to the C of the Si−C bond, indicating electron gain, leaving positive charges around the Si atom (i.e., electron loss). However, the resulting surface dipole is not only related to the Si−C bond. When the dipole induced by the adsorption of the aliphatic chain is calculated, it is found to be positive, contrary to the expectation based on having considered only the C atom closer to the surface. This

discrepancy can be readily explained by recognizing that, following the removal of a Hydrogen atom from one of the molecule's terminal groups and the subsequent formation of the Si–C bond, the molecule becomes asymmetric, and the charges located on the opposite terminal group (-CH_3 for alkyl and 1-alkynyl, and -CH_2 for 1-alkenyl moieties) contribute to the overall dipole. Our calculations demonstrate that the charge localized on the moiety's terminal group furthest from the surface is positive, thereby leading to the positive dipole induced by the adsorption of the moiety.

In Figures 4-8 it is also evident that the distance of the terminal group opposite to the surface from the interface of 1-alkynyl moieties decreases with respect to the number of C atoms. This is connected to the enhancement of the tilting angle as an effect of the triple C−C bond close to surface, as we have discussed above.

The dipole formed at the interface affects the thermionic transport at the Silicon/organic molecule/metal heterojunction, because of the Schottky Barrier (SB). Indeed, the SB depends on the surface dipole as follows: [10,16]

$$SB_e = \Phi - \chi - \psi \qquad (6)$$

$$SB_h = E_g - \Phi + \chi + \psi \qquad (7)$$

where Φ is the work function of the metal, χ is the electronic affinity of the semiconductor (Si), ψ is the energy step of the surface dipole in the equation (4), and E_g is the band gap of the semiconductor. SB_e and SB_h are the SB at zero bias of electrons and holes, respectively. From the equations (6) and (7) we see that positive surface dipoles reduce the SB of electrons and enhance the SB of holes. Upon the equations (6) and (7) and the values of the surface dipole reported in Tables 1-3, we can estimate how the SB depends on type and length of the aliphatic moiety. In Figure 9 we show how the electron and hole SBs of the Si−H/molecule/metal heterojunction change by varying adsorbed moiety when the metal is Hg by assuming Φ_{Hg} = 4.5 eV, χ_{Si} =4.06 eV [35] and E_g = 1.12 eV. When the adsorbate is an alkyl moiety, a slow variation of the SB is found with respect to N, with $SB_e \approx 0.3$ eV and $SB_h \approx 0.8$ eV. Attaching 1-alkenyl moieties, a monotonic and sensible variation of the SB is seen. For the adsorbate density of the interface in Figure 1, SB_e (SB_h) varies from 0.34 to 0.14 (0.78 to 0.98) eV for the chains with N=2 and N=10, respectively. We have different findings for 1-alkynyls. Specifically, SB_e (SB_h) of the C_2H 1-alkynyl moiety is 0.33 (0.79) eV. A change of 0.2 eV is obtained for C_4 and C_6, followed by a slow variation of 0.04 eV for C_8 and C_{10} (decrease of SB_e and increase of SB_h). To resume, among the investigated range of aliphatic chains, only 1-alkenyl moieties exhibit a regular and sensible variation of the SB by increasing N of the moiety. This is important when the electronic energetics at the interface must be tuned to control the thermionic transport in electronic devices. Of course, following the equation (4), by increasing the density of adsorbates the impact of the molecular dipole on the SB is enhanced. The qualitative variation of the SB for alkyl and 1-alkenyl moieties (i.e., SB_e decreases by increasing the length of the molecular chain) agrees with the experimental findings of Har-Lavan and co-authors. [36]

Computational Insights into the Energetics of Single C_2-C_{10} Aliphatic Moieties Adsorbed on Hydrogenated Silicon (111) Surface

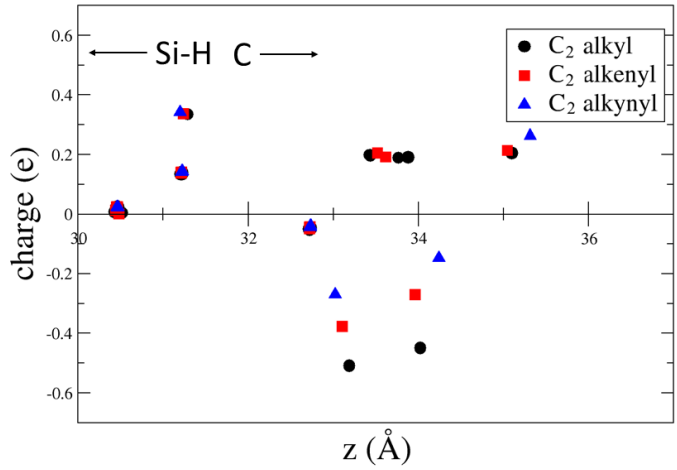

Figure 4. Difference between the Löwdin charge and the neutral atomic charge as a function of the z coordinate perpendicular to the surface for the C_2 alkyl, 1-alkenyl and 1-alkynyl moieties.

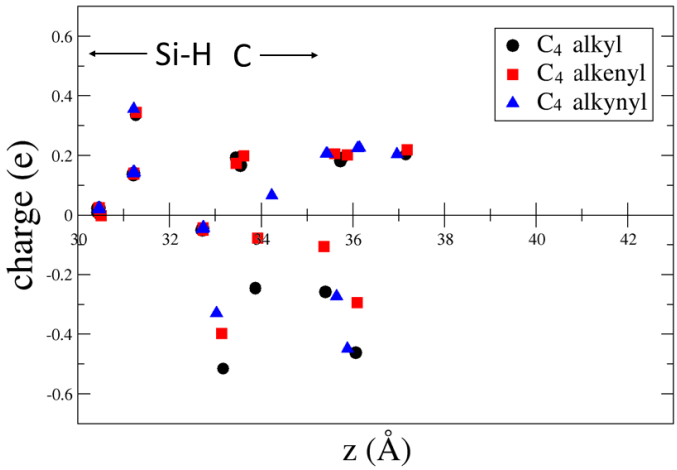

Figure 5. Difference between the Löwdin charge and the neutral atomic charge versus the z coordinate perpendicular to the surface for the C_4 alkyl, 1-alkenyl and 1-alkynyl moieties.

Computational Insights into the Energetics of Single C_2-C_{10} Aliphatic Moieties Adsorbed on Hydrogenated Silicon (111) Surface

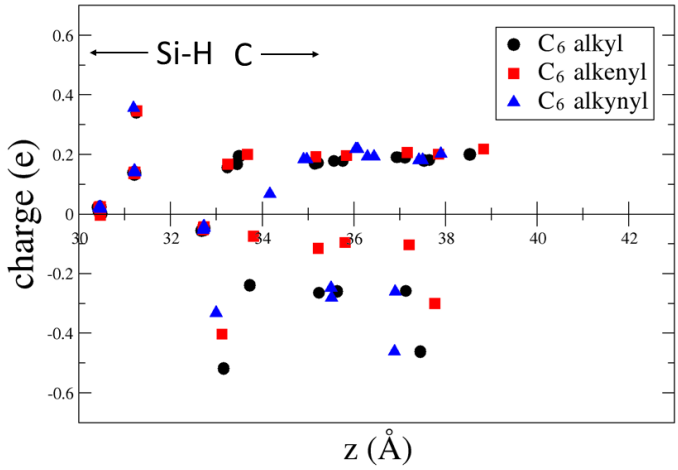

Figure 6. Difference between the Löwdin charge and the neutral atomic charge versus the z coordinate perpendicular to the surface for the C_6 alkyl, 1-alkenyl and 1-alkynyl moieties.

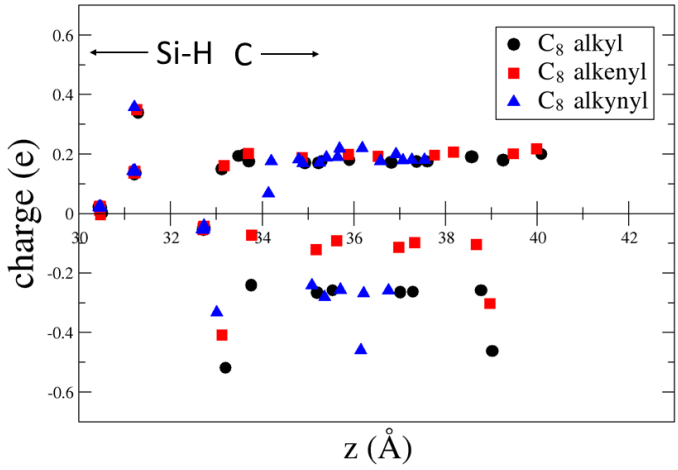

Figure 7. Difference between the Löwdin charge and the neutral atomic charge versus z coordinate perpendicular to the surface for the C_8 alkyl, 1-alkenyl and 1-alkynyl moieties.

Computational Insights into the Energetics of Single C_2-C_{10} Aliphatic Moieties Adsorbed on Hydrogenated Silicon (111) Surface

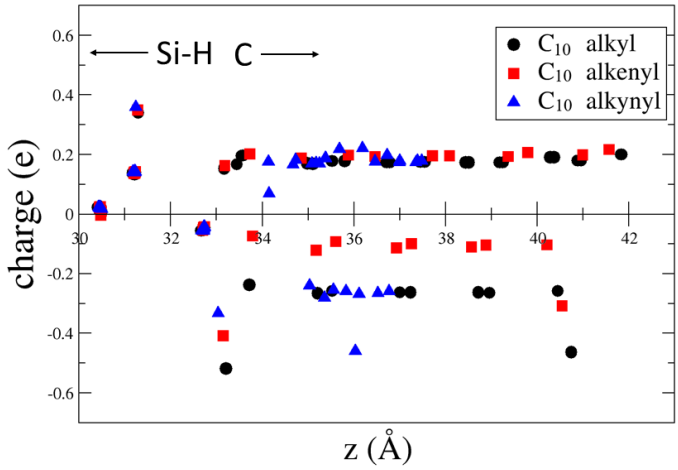

Figure 8. Difference between the Löwdin charge and the neutral atomic charge versus the z coordinate perpendicular to the surface for the C_{10} alkyl, 1-alkenyl and 1-alkynyl moieties.

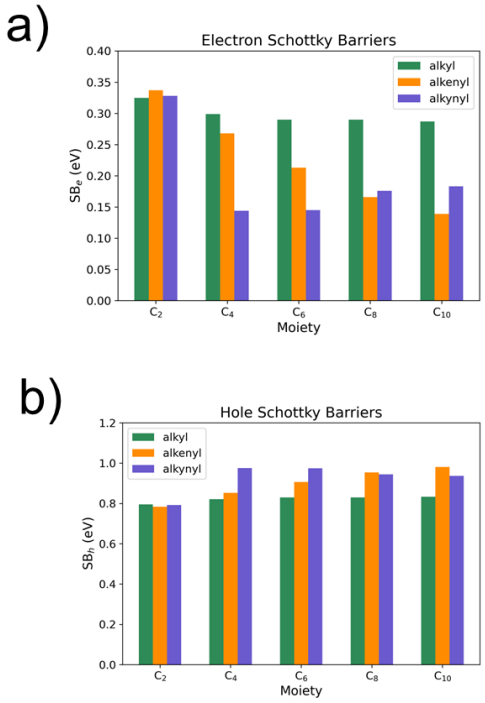

Figure 9. a) Electron and b) hole Schottky barriers of the alkyl, 1-alkenyl and 1-alkynyl modified Hg/H−Si(111) heterojunction calculated for the one moiety adsorbed per supercell model.

C. Interface energetics and tunnelling barriers

We determined the bands edges and the frontier orbital levels to investigate the energetics of the H−Si(111)/aliphatic chain heterointerface. We estimated the vacuum level of each adsorption configuration as the constant plane-averaged electrostatic energy in the vacuum gap far away from the top atomic layer, as shown in Figure S4. The valence and conduction band edges of the bulk Silicon have been aligned to that of the Silicon slab by overlapping the plane-averaged electrostatic energy in the central layers. We determined the HOMO and LUMO energies of the aliphatic moieties as the peaks of the projected DOS (PDOS) of the atomic orbitals associated to the organic molecule near the band gap (PDOS are shown in Figures S5-S19). The frontier orbital energy levels of alkyl, 1-alkenyl and 1-alkynyl moieties are compared to the band edges of bulk Si. The evolution of the energy levels is shown in Figures 10-12 as the C chain extends from C_2 to C_{10}. The same data are reported in Tables S1-S3. The energy shift of HOMO and LUMO with respect to valence and conduction band edges (E_V and E_C, respectively) are shown in Tables 1-3 and indicated as ΔHOMO (= E_V-HOMO) and ΔLUMO (= LUMO-E_C), respectively. ΔHOMO and ΔLUMO are the energy barrier for the tunnelling of holes and electrons, respectively.

The energy gap of the adsorbed alkyl and 1-alkynyl moieties has a weak dependence on the length of the chain. Indeed, the HOMO energy level of alkyls is almost independent on the moiety, while the LUMO energy level is a little bit more affected; ΔLUMO varies in a range of 0.23 eV centred around 3.2 eV that is wider than the variation of 0.04 eV of ΔHOMO centred around 0.81 eV. Conversely, the energy variation changing number of C atoms for occupied and unoccupied orbitals of the 1-alkynyl moieties are similar, because ΔLUMO and ΔHOMO vary in a range of 0.18 and 0.16 eV centred around 2.8 and 1.6 eV, respectively. Comparing alkyls and 1-alkynyls, we found that alkyl (1-alkynyl) moieties have the lowest hole (electron) energy barrier for tunnelling.

On the other side, the energy shift of HOMO and LUMO of 1-alkenyl moieties are more sensible to the length of the chain. The reason of this is that the energy gap of 1-alkenyls shrinks from 4.8 (C_2H_3) to 1.8 ($C_{10}H_{11}$) eV by increasing N, so that the frontier orbital energy levels get closer and closer to the band edges nearby. This involves that the values of ΔLUMO (ΔHOMO) of 1-alkenyl adsorbates change from 1.0 to 2.6 (0.2 to 1.6) eV, the variation being in a wide range of 1.41 (1.58) eV. The 1-alkenyl moieties originate in absolute the lowest energy barriers by increasing the length of the molecular chain. The adsorption of the C_{10} 1-alkenyl moiety reduces the tunnelling barrier the most and enhance the transport related to this charge transfer mechanism. Although nonlocal functionals still underestimate the energy gap of molecules and semiconductors, it is interesting to observe that the electron tunnelling barrier of C_9 1-alkenyl moiety in the experiments is found to be around 1 eV, [37] in nice agreement with the values of 1.2 and 1.0 eV for C_8 and C_{10} 1-alkenyl moieties, respectively, obtained in the present work.

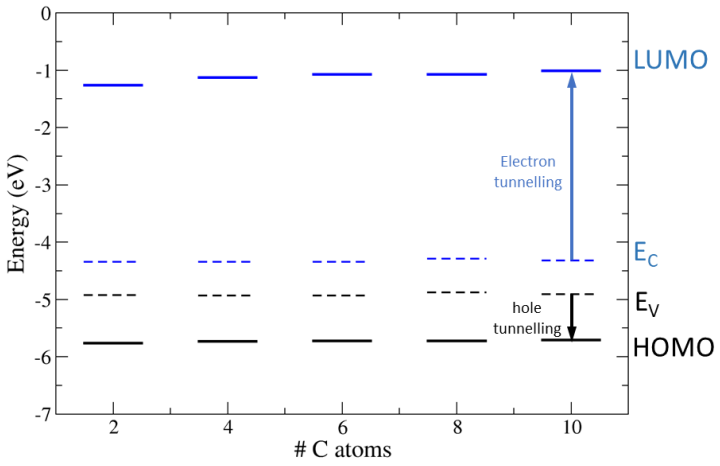

Figure 10. Valence (E_V) and conduction (E_C) band edges (dashed lines) of bulk Silicon and HOMO/LUMO energy levels (full lines) of alkyl moieties (black: occupied states; blue: unoccupied states). The electron and hole tunnelling barriers are evidenced as blue and black arrows, respectively, for the C_{10} chain. The vacuum level is set to 0 eV.

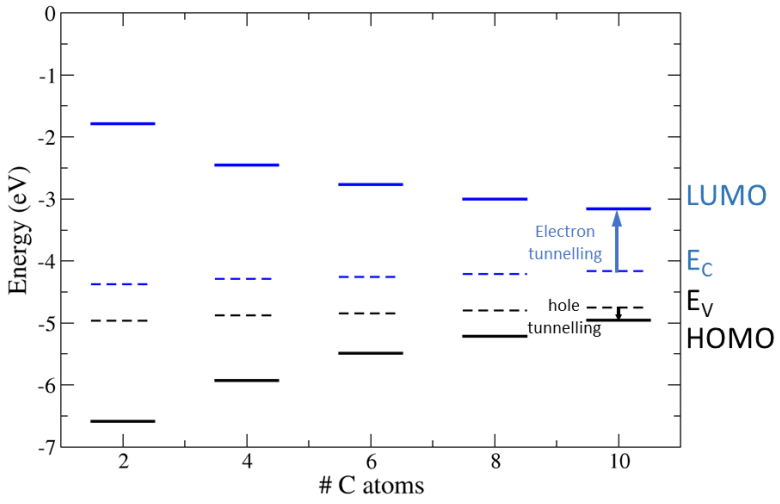

Figure 11. Valence (E_V) and conduction (E_C) band edges (dashed lines) of bulk Silicon and HOMO/LUMO energy levels (full lines) of 1-alkenyl moieties (black: occupied states; blue: unoccupied states). The electron and hole tunnelling barriers are evidenced as blue and black arrows, respectively, for the C_{10} chain. The vacuum level is set to 0 eV.

Computational Insights into the Energetics of Single C_2-C_{10} Aliphatic Moieties Adsorbed on Hydrogenated Silicon (111) Surface

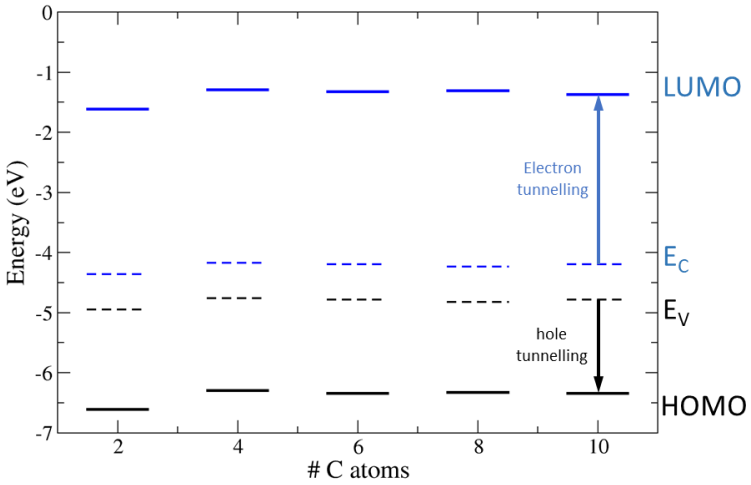

Figure 12. Valence (E_V) and conduction (E_C) band edges (dashed lines) of bulk Silicon and HOMO/LUMO energy levels (full lines) of 1-alkynyl moieties (black: occupied states; blue: unoccupied states). The electron and hole tunnelling barriers are evidenced as blue and black arrows, respectively, for the C_{10} chain. The vacuum level is set to 0 eV.

Table 4. Ab initio tunnelling barriers for holes (ΔHOMO) and electrons (ΔLUMO), of the alkyl moieties adsorbed on the H−Si(111) surface.

Chain	ΔHOMO (eV)	ΔLUMO (eV)
C_2	0.83	3.08
C_4	0.80	3.21
C_6	0.79	3.28
C_8	0.83	3.23
C_{10}	0.81	3.31

Table 5. Ab initio tunnelling barriers for holes (ΔHOMO) and electrons (ΔLUMO) of the 1-alkenyl moieties adsorbed on the H−Si(111) surface.

Chain	ΔHOMO (eV)	ΔLUMO (eV)
C_2	1.63	2.59
C_4	1.05	1.84
C_6	0.65	1.49
C_8	0.41	1.21
C_{10}	0.21	1.01

Table 6. Ab initio tunnelling barriers for holes (ΔHOMO) and electrons (ΔLUMO) of the 1-alkynyl moieties adsorbed on the H−Si(111) surface.

Chain	ΔHOMO (eV)	ΔLUMO (eV)
C_2	1.67	2.75
C_4	1.54	2.88
C_6	1.56	2.87
C_8	1.51	2.93
C_{10}	1.56	2.83

E. Conclusions

In the present work we have investigated the effects of adsorption of single aliphatic moieties on H–Si(111) surfaces. A wide range of possible adhesion configurations of alkyl (C_nH_{2n+1}), 1-alkenyl (C_nH_{n+1}) and 1-alkynyl (C_2H_1, C_nH_{2n-3} for n>2) moieties has been explored and the structural characterization in the minimal energy geometries has been reported. The presence of single, double or triple C−C bond near the surface has different impact on the Silicon/molecule interface energetics. The 1-alkynyl moieties have the higher dissociation energy, followed by the 1-alkenyl and alkyl moieties. The trend of the tilting of the molecular axis $\mathbf{C_1C_N}$ of 1-alkynyl moieties is to increase with the number of C atoms. Indeed, the shortest 1-alkynyl adsorbate is almost perpendicular to the surface, while the longest one exhibit the highest tilting angle.

The surface dipole influences the SB at the semiconductor/organic/metal interface given the work function of the metal and the electronic affinity of the semiconductor and affects the thermionic transport. Simple considerations on the Pauling electronegativity on the Si−C bond wrongly predict the surface dipole to be negative. Rather, to correctly predict the direction of the dipole the distribution of the charge along the entire aliphatic chain should be considered. We showed that the positive charge localized on the moiety's terminal group opposite to the surface gives rise to the positive dipole (i.e., positive charge pointing outward and negative charge pointing inward). The alkyl and 1-alkynyl adsorbates give almost constant SB when the aliphatic chain is longer than N=2. Instead, the 1-alkenyl moieties exhibit a regular and sensible variation of the SB by increasing N of the hydrocarbon chain. This is significant to tune the electronic energetics at the interface.

We calculated the alignment of the frontier molecular orbital energy levels to the bands of the semiconductor to get insights into the tunnelling transport. Comparing alkyl and 1-alkynyl moieties, we found that the alkyl (1-alkynyl) chains have the lowest hole (electron) energy barrier for tunnelling, with weak dependence on N. Instead, the 1-alkenyl moieties give rise in absolute to the lowest energy barriers, whose height decreases by increasing N. Indeed, the C_{10} 1-alkenyl moiety reduces the tunnelling energy barrier until to 1 eV for electrons and 0.2 eV for holes, and we predict it to enhance the most the tunnelling mechanism. The range of values we found is in good agreement with the available experimental measurements. In monolayers, broadening of the energy levels is present due to the interaction between adsorbates and substrate and among molecules.

The applicability of our approach and findings extends beyond thermionic and tunnelling transport in electronic devices. Indeed, our results can also be useful in other contexts, such as

tuning of electron or hole transport layers in photovoltaic devices or regulation of the interface energetics in water-splitting applications. The present study can be expanded by pursuing the following objectives: investigation of longer aliphatic chains until C_{18}; adsorption on other relevant Si surfaces as Si(110) and Si(100); usage of the ab initio calculated parameters as input of phenomenological models. The findings for single moiety adsorption presented in this work paves the way to further studies targeting the adsorption of multiple moieties forming monolayers. This target holds significant implications for the development of next-generation electronics, sensors, and photovoltaic systems, highlighting the potential of aliphatic chains surface functionalization in enhancing Silicon's already impressive capabilities.

ACKNOWLEDGMENTS

This work was supported by the European Union through the Next Generation EU funds through the Italian MUR National Recovery and Resilience Plan, Mission 4 Component 2 – Investment 1.4 – National Center for HPC, Big Data and Quantum Computing – CUP I33C22001270007. The computing resources and the related technical support used for this work have been provided by CRESCO/ENEAGRID High Performance Computing infrastructure and its staff. [38] CRESCO/ENEAGRID High Performance Computing infrastructure is funded by ENEA, the Italian National Agency for New Technologies, Energy and Sustainable Economic Development and by Italian and European research projects, see http://www.cresco.enea.it/english for information. The authors acknowledge the extensive use of the ENEA FARO facility and the support of its management team. [39] The authors thank prof. Mohammed Y. Bashouti for useful discussions.

REFERENCES

(1) Har-Lavan, R.; Ron, I.; Thieblemont, F.; Cahen, D. Toward metal-organic insulator-semiconductor solar cells, based on molecular monolayer self-assembly on n-Si. *Appl. Phys. Lett.* **2009**, *94* (4), 043308. https://doi.org/10.1063/1.3076115.

(2) Maldonado, S.; Knapp, D.; Lewis, N. S. Near-Ideal Photodiodes from Sintered Gold Nanoparticle Films on Methyl-Terminated Si(111) Surfaces. *J. Am. Chem. Soc.* **2008**, *130* (11), 3300. https://doi.org/10.1021/ja800603v.

(3) Gal, D.; Sone, E.; Cohen, R.; Hodes, G.; Libman, J.; Shanzer, A.; Schock, H. W.; Cahen, D. Engineering the interface energetics of solar cells by grafting molecular properties onto semiconductors. *Proc. Indian Acad. Sci. Chem. Sci.* **1997**, *109* (6), 487.

(4) Visoly-Fisher, I.; Sitt, A.; Wahab, M.; Cahen, D. Molecular Adsorption-Mediated Control over the Electrical Characteristics of Polycrystalline CdTe/CdS Solar Cells. *ChemPhysChem* **2005**, *6* (2), 277. https://doi.org/10.1002/cphc.200400392.

(5) Page, M.; Niitsoo, O.; Itzhaik, Y.; Cahen, D.; Hodes, G. Copper sulfide as a light absorber in wet-chemical synthesized extremely thin absorber (ETA) solar cells. *Energy Environ. Sci.* **2009**, *2* (2), 220. https://doi.org/10.1039/B813740D.

(6) Wu, D. G.; Ashkenasy, G.; Shvarts, D.; Ussyshkin, R. V.; Naaman, R.; Shanzer, A.; Cahen, D. Novel NO Biosensor Based on the Surface Derivatization of GaAs by "Hinged" Iron porphyrins. *Angew. Chem., Int. Ed.* **2000**, *39* (24), 4496.

(7) Stern, E.; Wagner, R.; Sigworth, F. J.; Breaker, R.; Fahmy, T. M.; Reed, M. A. Importance of the Debye Screening Length on Nanowire Field Effect Transistor Sensors. *Nano Lett.* **2007**, *7* (11), 3405. https://doi.org/10.1021/nl071792z.

(8) Cattani-Scholz, A.; Pedone, D.; Dubey, M.; Neppl, S.; Nickel, B.; Feulner, P.; Schwartz, J.; Abstreiter, G.; Tornow, M. Organophosphonate-Based PNA-Functionalization of Silicon

Nanowires for Label-Free DNA Detection. *ACS Nano* **2008**, *2* (8), 1653. https://doi.org/10.1021/nn800136e.

(9) Peng, G.; Tisch, U.; Haick, H. Detection of Nonpolar Molecules by Means of Carrier Scattering in Random Networks of Carbon Nanotubes: Toward Diagnosis of Diseases via Breath Samples. *Nano Lett.* **2009**, *9* (4), 1362. https://doi.org/10.1021/nl8030218.

(10) Vilan, A.; Cahen, D. Chemical Modification of Semiconductor Surfaces for Molecular Electronics. *Chem. Rev.* **2017**, *117* (5), 4624. https://doi.org/10.1021/acs.chemrev.6b00746.

(11) Bashouti, M. Y.; Pietsch, M.; Brönstrup, G.; Sivakov, V.; Ristein, J. Heterojunction Based Hybrid Silicon Nanowire Solar Cell: Surface Termination, Photoelectron and Photoemission Spectroscopy Study. *Prog. Photovolt: Res. Appl.* **2014**, *22* (9), 1050-1061. https://doi.org/10.1002/pip.2315.

(12) Shalabny, A.; Buonocore, F.; Celino, M.; Zhang, L.; Sardashti, K.; Härth, M.; Schubert, D. W.; Bashouti, M. Y. Enhancing the Electronic Properties of VLS-Grown Silicon Nanowires by Surface Charge Transfer. *Appl. Surf. Sci.* **2022**, *599*, 153957. https://doi.org/10.1016/j.apsusc.2022.153957.

(13) Shalabny, A.; Buonocore, F.; Celino, M.; Shalev, G.; Zhang, L.; Wu, W.; Li, P.; Arbiol, J.; Bashouti, M. Y. Semiconductivity Transition in Silicon Nanowires by Hole Transport Layer. *Nano Lett.* **2020**, *20* (11), 8369–8374. https://doi.org/10.1021/acs.nanolett.0c03543.

(14) Harilal, S.; Sadhujan, S.; Zhang, K.; Shalabny, A.; Buonocore, F.; Ferrucci, B.; Giusepponi, S.; Celino, M.; Bashouti, M. Y. Uniform Tendency of Surface Dipoles Across Silicon Doping Levels and Types of H-Terminated Surfaces. *Adv. Electron. Mater.* **2024**, 10 (10), 2300873. https://doi.org/10.1002/aelm.202300873.

(15) Linford, M. R.; Chidsey, C. E. D. Alkyl monolayers covalently bonded to silicon surfaces. *J. Am. Chem. Soc.* **1993**, *115* (26), 12631. https://doi.org/10.1021/ja00079a071.

(16) Vilan, A.; Yaffe O.; Biller, A.; Salomon, A.; Kahn, A.; Cahen, D. Molecules on Si: Electronics with Chemistry. *Adv. Mater.* **2010**, *22*, 140. https://doi.org/10.1002/adma.200901834.

(17) Bashouti, M. Y.; Garzuzi, C. A.; de la Mata, M.; Arbiol, J.; Ristein, J.; Haick, H.; Christiansen, S. Role of Silicon Nanowire Diameter for Alkyl (Chain Lengths C_1–C_{18}) Passivation Efficiency through Si–C Bonds. *Langmuir* **2015**, *31* (8), 2430-2437. https://doi.org/10.1021/la5047244.

(18) Pujari, S. P.; Filippov, A. D.; Gangarapu, S.; Zuilhof, H. High-Density Modification of H-Terminated Si(111) Surfaces Using Short-Chain Alkynes. *Langmuir* **2017**, *33* (51), 14599-14607. https://doi.org/10.1021/acs.langmuir.7b03683.

(19) Zhang, L.; Wesley, K.; Jiang, S. Molecular Simulation Study of Alkyl Monolayers on Si(111). *Langmuir* **2001**, *17* (20), 6275. https://doi.org/10.1021/la0106337.

(20) Yuan, S.; Zhang, Y.; Li, Y.; Xu, G. Molecular simulation study of different monolayers on Si (111) surface. *Colloids Surf., A* **2004**, *242* (1–3), 129-135. https://doi.org/10.1016/j.colsurfa.2004.03.031.

(21) Scheres, L.; Rijksen, B.; Giesbers, M.; Zuilhof, H. Molecular Modeling of Alkyl and Alkenyl Monolayers on Hydrogen-Terminated Si(111). *Langmuir* **2011**, *27* (3), 972-980. https://doi.org/10.1021/la104705b.

(22) Gala, F.; Zollo, G. Functionalization of Hydrogenated (111) Silicon Surface with Hydrophobic Polymer Chains. *Phys. Rev. B* **2011**, *84* (19), 195323. https://doi.org/10.1103/PhysRevB.84.195323.

(23) Arefi, H. H.; Nolan, M.; Fagas, G. Density Functional Theory with van der Waals Corrections Study of the Adsorption of Alkyl, Alkylthiol, Alkoxyl, and Amino-Alkyl Chains on the H:Si(111) Surface. *Langmuir* **2014**, *30* (44), 13255-13265. https://doi.org/10.1021/la502488c.

(24) Soria, F. A.; Paredes-Olivera, P.; Patrito, E. M. Chemical Stability Toward O_2 and H_2O of Si(111) Grafted with —CH_3, —$CH_2CH_2CH_3$, —$CHCHCH_3$, and —$CCCH_3$. *J. Phys. Chem. C* **2015**, *119* (1), 284-295. https://doi.org/10.1021/jp508728v.

(25) Arefi, H. H.; Nolan, M.; Fagas, G. Role of the Head and/or Tail Groups of Adsorbed –[$X^{head\ group}$]–Alkyl–[$X^{tail\ group}$] [X = O(H), S(H), $NH_{(2)}$] Chains in Controlling the Work Function of the Functionalized H:Si(111) Surface. *J. Phys. Chem. C* **2015**, *119* (21), 11588-11597. https://doi.org/10.1021/acs.jpcc.5b01177

(26) Scheres, L.; Giesbers, M.; Zuilhof, H. Self-Assembly of Organic Monolayers onto Hydrogen-Terminated Silicon: 1-Alkynes Are Better Than 1-Alkenes. *Langmuir* **2010**, *26* (13), 10924-10929. https://doi.org/10.1021/la100858q.

(27) Giannozzi, P.; Baroni, S.; Bonini, N.; Calandra, M.; Car, R.; Cavazzoni, C.; Ceresoli, D.; Chiarotti, G. L.; Cococcioni, M.; Dabo, I.; Dal Corso, A.; Fabris, S.; Fratesi, G.; de Gironcoli, S.; Gebauer, R.; Gerstmann, U.; Gougoussis, C.; Kokalj, A.; Lazzeri, M.; Martin-Samos, L.; Marzari, N.; Mauri, F.; Mazzarello, R.; Paolini, S.; Pasquarello, A.; Paulatto, L.; Sbraccia, C.; Scandolo, S.; Sclauzero, G.; Seitsonen, A. P.; Smogunov, A.; Umari, P.; Wentzcovitch, R. M. QUANTUM ESPRESSO: A Modular and Open-Source Software Project for Quantum Simulations of Materials. *J. Phys.: Condens. Matter* **2009**, *21* (39), 395502. https://doi.org/10.1088/0953-8984/21/39/395502.

(28) Giannozzi, P.; Andreussi, O.; Brumme, T.; Bunau, O.; Buongiorno Nardelli, M.; Calandra, M.; Car, R.; Cavazzoni, C.; Ceresoli, D.; Cococcioni, M.; Colonna, N.; Carnimeo, I.; Dal Corso, A.; de Gironcoli, S.; Delugas, P.; DiStasio, R. A.; Ferretti, A.; Floris, A.; Fratesi, G.; Fugallo, G.; Gebauer, R.; Gerstmann, U.; Giustino, F.; Gorni, T.; Jia, J.; Kawamura, M.; Ko, H.-Y.; Kokalj, A.; Küçükbenli, E.; Lazzeri, M.; Marsili, M.; Marzari, N.; Mauri, F.; Nguyen, N. L.; Nguyen, H.-V.; Otero-de-la-Roza, A.; Paulatto, L.; Poncé, S.; Rocca, D.; Sabatini, R.; Santra, B.; Schlipf, M.; Seitsonen, A. P.; Smogunov, A.; Timrov, I.; Thonhauser, T.; Umari, P.; Vast, N.; Wu, X.; Baroni, S. Advanced Capabilities for Materials Modelling with QUANTUM ESPRESSO. *J. Phys.: Condens. Matter* **2017**, *29* (46), 465901. https://doi.org/10.1088/1361-648X/aa8f79.

(29) Berland, K.; Hyldgaard, P. Exchange Functional That Tests the Robustness of the Plasmon Description of the van der Waals Density Functional. *Phys. Rev. B* **2014**, *89* (3), 035412. https://doi.org/10.1103/PhysRevB.89.035412.

(30) Wang, X.; Esfarjani, K.; Zebarjadi, M. First-Principles Calculation of Charge Transfer at the Silicon–Organic Interface. *J. Phys. Chem. C* **2017**, *121* (29), 15529-15537. https://doi.org/10.1021/acs.jpcc.7b03275.

(31) Vanderbilt, D. Soft Self-Consistent Pseudopotentials in a Generalized Eigenvalue Formalism. *Phys. Rev. B* **1990**, *41* (11), 7892-7895. https://doi.org/10.1103/PhysRevB.41.7892.

(32) Bengtsson, L. Dipole Correction for Surface Supercell Calculations. *Phys. Rev. B* **1999**, *59* (19), 12301. https://doi.org/10.1103/PhysRevB.59.12301.

(33) Marchio, S.; Buonocore, F.; Giusepponi, S.; Celino, M. Density Functional Theory Study of Silicon Nanowires Functionalized by Grafting Organic Molecules. *Materials Cloud Archive* **2024**, *81*. https://doi.org/10.24435/materialscloud:15-fs.

(34) Buonocore, F.; di Matteo, A. Energetic of molecular interface at metal-organic heterojunction: the case of thiophenethiolate chemisorbed on Au(111). A. *Theor. Chem. Acc.* **2009**, *124*, 217. https://doi.org/10.1007/s00214-009-0602-4.

(35) Haj-Yahia, A.-E.; Yaffe, O.; Bendikov, T.; Cohen, H.; Feldman, Y.; Vilan, A.; Cahen, D. Substituent Variation Drives Metal/Monolayer/Semiconductor Junctions from Strongly Rectifying to Ohmic Behavior. *Adv. Mater*. **2013**, *25*, 702−706.

(36) Har-Lavan, R.; Yaffe, O.; Joshi, P.; Kazaz, R.; Cohen, H.; Cahen, D. Ambient Organic Molecular Passivation of Si Yields Near-Ideal, Schottky-Mott Limited Junctions. *AIP Adv.* **2012**, *2* (1), 012164.

(37) Aragonès, A.; Darwish, N.; Ciampi, S.; Sanz, F.; Gooding, J. J.; Dìez-Pérez, I. Single-Molecule Electrical Contacts on Silicon Electrodes Under Ambient Conditions. *Nat. Commun.* **2017**, *8*, 15056. https://doi.org/10.1002/adma.201203028.

(38) Iannone, F.; et al. CRESCO ENEA HPC Clusters: A Working Example of a Multifabric GPFS Spectrum Scale Layout. 2019 International Conference on High Performance Computing & Simulation (HPCS), Dublin, Ireland, 2019, 1051. https://doi.org/10.1109/HPCS48598.2019.9188135.

(39) Mariano, A.; et al. Fast Access to Remote Objects 2.0: A Renewed Gateway to ENEAGRID Distributed Computing Resources. *Future Gener. Comput. Syst.* **2019**, *94*, 920–928. https://doi.org/10.1016/j.future.2018.12.032.